Journal of Biomedical Optics

SPIEDigitalLibrary.org/jbo

Fast multi-spectral imaging technique for detection of circulating endothelial cells in human blood samples

Ihor V. Berezhnyy
Svitlana Y. Berezhna

SPIE

Fast multi-spectral imaging technique for detection of circulating endothelial cells in human blood samples

Ihor V. Berezhnyy[a] and Svitlana Y. Berezhna[b]
[a]Physical Optics Corporation, Torrance, California 90501
[b]The Scripps Research Institute, Department of Molecular Biology, La Jolla, California 92037

Abstract. The appearance of non-blood cells circulating in human peripheral bloodstream indicates an abnormal condition. One important category of these cells is circulating endothelial cells (CECs) shed by compromised blood vessels. Clinical applications that measure the blood level of CECs are hindered due to a lack of standardized instruments. The major challenge in detecting circulating non-blood cells is their extreme scarcity; 1 in 10^6 to 10^7. Described here is a new method for detection of rare cells in blood samples deposited on the adhesive microscopic slides and immunostained with distinct fluorescent markers. The key novelty of the proposed approach is an intelligent search principle and a dual-mode scanner to implement this principle. To begin, a fast scanning that uses a single beam is performed in the spectral channel where only rare cells produce florescence. Once a target cell is registered, the scanner switches on the imaging mode, auto-focuses and then records images in multiple spectral channels at the selected area. The instrument runs in repetitive cycles until the entire slide is scanned. The technology has been validated via detection of human umbilical vein endothelial cells spiked into human blood samples. In addition, the operational principle can be adapted for detection of other types of rare cells in blood. [DOI: 10.1117/1.JBO.17.8.081404]

Keywords: clinical imaging; rare cells; circulating endothelial cells; blood; cardiovascular diseases; cancer.

Paper 11671SS received Nov. 16, 2011; revised manuscript received Mar. 2, 2012; accepted for publication Mar. 13, 2012; published online May 16, 2012.

1 Introduction

More than a century ago, Australian physician Thomas Ashworth described "a case of cancer in which cells similar to those in the tumours were seen in the blood."[1] In that study, tumor cells in the bloodstream were discovered by examining blood samples under the light microscope and spotting a population of cells with a morphology different from the blood cells. Further examination of that rare cell population revealed that their morphology is similar to those from the tumor. Currently, investigation of circulating tumor cells (CTCs) has evolved into the burgeoning field of cancer research with multiple techniques proposed for detection, isolation and molecular characterization of CTCs.[2,3]

Less well characterized but no less important are circulating endothelial cells (CECs). These cells are shed from the endothelium, a thin layer of cells that line the interior blood vessel surface. In healthy individuals, endothelial cells remain in the blood vessel wall with a very low level of cell loss into the blood (<5 cells/ml of blood). Endothelium damage causes endothelial cell detachment, resulting in increased numbers of CECs in the bloodstream (~8 to 50 cells/ml) observed for patients with various cardiovascular diseases.[4] An elevated number of CECs was also detected in patients suffering from other diseases with vascular involvement, such as cancer.[5] The CECs have been recognized as noninvasive biomarkers reflecting the dynamics between endothelial injury and repair, and are therefore considered as promising prognostic and diagnostic indicators of cardiovascular diseases.[6–8]

A critical impediment for broad implementation of blood tests for different types of rare cells into clinical practice is the lack of generally accepted robust instruments and assays for their detection and enumeration. In fact, in the absence of any established standards with which to evaluate various technologies and define their absolute accuracy, sensitivity and specificity of rare cell detection, the development of instrumental tools presents a significant challenge. The ultimate technology must be capable of isolating and preserving intact any predefined population of rare cells (1 cell from 10^6 to 10^7) in a pure, sensitive, speedy and cost-effective manner. A variety of currently proposed approaches utilizes either the physical properties (size, charge, density, etc.), expression of biomarkers or functional characteristics to discriminate the population of the rare cells from the rest of blood cells. Although none of the existing approaches constitute the optimal platform for rare cell isolation, they all undergo continuous testing and refinement, and provide a basis for the next generation of clinically viable methods.[3]

One key approach for rare cell detection is microscopic inspection of blood samples deposited on the glass slides. This method, combined with immunochemical staining of the cells to visualize the presence of specific markers, holds an important advantage of relying on multiple parameters for identification and characterization of the specific population of interest. The difficulty, however, of high-throughput microscopic imaging when applied to rare event detection is the need to acquire and analyze extremely large sets of images, most of which contain no information about the population of interest. Therefore, conventional multicolor imaging flow cytometry becomes

Address all correspondence to: Svitlana Y. Berezhna, The Scripps Research Institute, 10550 N. Torrey Pines Road, La Jolla, California 92037. Tel: +1 8587842912; Fax: +1 8587849067; E-mail: berezhna@scripps.edu.

0091-3286/2012/$25.00

inconveniently slow to screen for a statistically valid number of rare cells.[3,9] To overcome this difficulty, a possible approach is to combine microscopic imaging with sample enrichment. In this two-step methodology, silicon posts coated with specific antibodies and assembled in microchips[10,11] or immuno-magnetic beads are first used to capture and pull down rare cells from the blood sample, which are subsequently examined by imaging microscopy for a final assessment. Currently, the only FDA-approved technology for CTCs or CECs detection (CellSearch®) uses such an immuno-magnetic enrichment procedure combined with imaging microscopy. The sensitivity of this enrichment-based methodology, however, has proven to be low, finding none to very few CTCs in most patients.[3,12]

Most recently, a fast laser scanning imaging technology that detects CTCs without the enrichment step[9,13,14] has been developed and demonstrated through the comparison studies of the blood samples taken from the same patients that CellSearch® assay produces a systematically smaller number of CTCs per ml of blood.[15] Currently, this advanced imaging method is recognized as a promising detection platform due to its specificity, accuracy and a simple sample preparation procedure.[15] However, the existing model of the fast laser scanner requires elaborate and expensive equipment that includes an opto-mechanical system with a precisely rotating mirror, f-theta field lens and a fiber optic bundle for light collection.[9,14]

We have devised an inexpensive and efficient multi-spectral optical imaging method for fast and accurate detection of rare cells in blood samples deposited on the adhesive microscopic slides. This new technique is based on an immuno-fluorescence detection principle, similar to the fast laser scanning method. The proposed technology, however, significantly reduces data recording time and a number of collected images due to the unique intelligent search principle. The instrument can be built on commercially available lower-end microscopes and involves relatively simple and affordable modifications. The operational principle, optical design and test experiments are presented in the following sections. The initial experiments demonstrated feasibility of the proposed concept for creating the next generation platform for rare cell detection in clinical settings.

2 Operational Principle

A general operational principle of the proposed technology and its workflow is schematically illustrated in Fig. 1. The technology comprises two major operational segments. A first stage includes processing blood samples and preparing blood smear slides. The prepared slides can either be scanned and analyzed immediately upon preparation, or frozen until further analysis. A second stage includes scanning slides on the dual-mode scanner and recording a set of images in multiple spectral channels. Presumably, collected data sets contain all potential rare cells existing on the slide along with some artifacts. All final classifications and quantifications of the rare cell population of interest are performed by a trained operator with the help of ontology-based software that identifies CECs or CTCs based on multiple selection criteria. Finally, the system generates a total number report and an image gallery of all detected rare cells.

A protocol for blood sample processing and slide preparation procedure implemented in the current technology have been developed, validated and described in details elsewhere.[9,13] In brief, a blood sample is collected via venipuncture into an ethylenediaminetetraacetic acid (EDTA) tube, kept on ice before processing, and then rocked for 5 min prior to performing a white blood cell count. Based on the white blood cell number, a certain volume of blood undergoes red blood cell lysis.

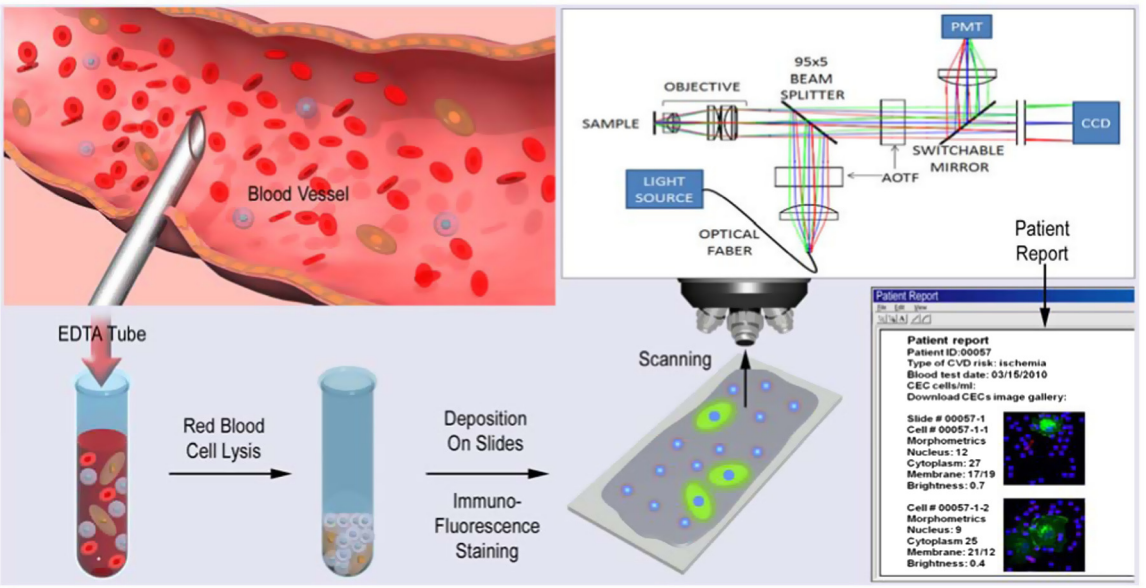

Fig. 1 A workflow of the proposed technology for rare cell detection. Blood is collected via venipuncture into an EDTA tube. Leukocyte count is performed and a certain amount of the sample undergoes red blood cell lysis. The white blood cell pellet containing rare cells is resuspended in the physiological buffer. The cells in suspension are evenly distributed on the microscopic adhesive slides at a density of $\sim 3.5 \times 10^6$ cells/slide. After cells adhere to the slides, the sample undergoes immuno-fluorescence staining. A specific set of fluorescently labeled antibodies is selected to enable discrimination of rare cells from leukocytes. Prepared slides are scanned using the multi-spectral imaging scanner, which generates a set of multicolor images collected only in the areas potentially containing target cells of interest. An operator, with the help of the ontology-based sure-search software performs image analysis and provides a patient's report. The report contains a number of rare cells per milliliter of blood, their images and morphometric characteristics.

The white blood cells pellet containing CECs and/or CTCs is resuspended in the physiological buffer. All cells in the suspension are evenly distributed on the microscopic adhesive slides and incubated for sufficient attachment. Special surface coating on the slide provides binding conditions that enable maximal retention of live cells, such that each slide can hold approximately three million nucleated cells.[9,15] The cells captured on the slide are fixed, permeabilized, pre-blocked for prevention of non-specific binding and then undergo immuno-fluorescence staining. A set of fluorescently labeled antibodies used for immunostaining typically includes positive and negative selection markers to provide reliable discrimination of CTCs or CECs from leukocytes, making the cells on the slides ready for imaging and analysis.

3 Optical System of Fast Multi-Spectral Imaging Scanner

The approach to rare cell detection devised here exploits scarcity of these cells and significantly reduces time for their screening, identification and enumeration without compromising detection accuracy. The instrument can function in two independent scanning modes that are combined by software to execute a specific operational regime. A smart search principle implemented in this instrument suggests that at the start, the instrument performs a fast scanning with a narrow single beam in the spectral channel where only rare cells can produce fluorescence. Upon registering a signal in this channel set above a pre-set threshold level, the instrument pauses and switches on the high-resolution imaging mode. In this mode, the scanner switches to a higher numerical aperture objective lens and performs autofocusing to secure high-quality of imaging data. Next, a set of high-resolution images in multiple spectral channels is recorded at several adjacent quadrants surrounding the selected spot of interest on the slide. In this way, instead of subsequently imaging all the cells deposited on the slide (the majority of which are not the cells of interest) and performing multiple cycles of recording, storing and analyzing immense datasets, the instrument collects data only at the sites that potentially contain rare cell candidates. This intelligent operational mode dramatically reduces number of recorded images and the instrument's running time. An additional advantage of performing fast pre-screening with a narrow beam is to reduce photo-bleaching of fluorescent markers before imaging.

For maximum flexibility, the instrument can be equipped with several objective lenses. One possible set is three Nikon Plan Apochromat objectives, 10×, 0.45 N.A., 20×, 0.75 N.A., and 40× C, 0.95 N.A. Fast scanning is performed with a 10× objective providing a larger field of view. In the imaging mode, the system is programmed to switch to a 20×, 0.75 N.A. objective characterized by the higher resolution and larger signal collection. Per request, an operating algorithm can be programmed so that in certain raster areas on the slide the cells are imaged with a 40× C, 0.95 N.A. objective and so enabling detection of fine morphological features of the selected cells.

An optical diagram of the system is schematically shown in Fig. 2. An excitation beam from the multi-spectral light source is coupled to the optical fiber and shaped by a lens before entering an acousto-optical tunable filter (AOTF). The first AOTF in the system controls the wavelenght of the excitation beam. Upon passing through the AOTF, the beam is reflected by the beam splitter in the perpendicular direction and enters the objective lens. All objectives are placed on the rotating turret controlled by the electronics. The turret is capable of controlled movement along the optical axis. The objective focuses the excitation beam on the sample, which is positioned on the XY-translational stage. A combined fluorescence signal produced by several fluorophores in the sample is collected by the same objective, passes through the beam splitter and is separated into individual spectral channels by the second AOTF placed in the detection channel. An electronically switchable mirror directs the fluorescence signal either to the photomultiplier tube (PMT) (in the fast scanning mode) or to the charge-coupled device (CCD) camera (in the imaging mode) for detection.

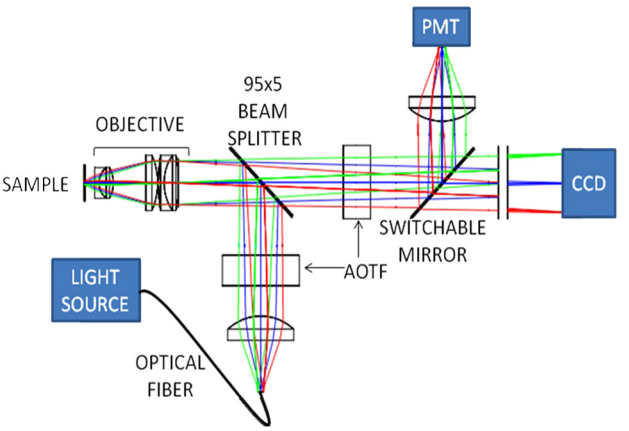

Fig. 2 An optical scheme of the fast multi-spectral dual-mode scanner. An excitation beam from the multi-spectral light source is coupled to the optical fiber. At the fiber output, the beam is shaped by the lens and enters an acousto-optical tunable filter (AOTF). A first AOTF controls the wavelenght of the excitation beam. The beam splitter (95 × 5 Beam Splitter) directs the excitation beam to the objective, which focuses the beam on the sample. The sample is placed on the XY-translational stage. All objectives are positioned on the rotating turret controlled by the electronics. Fluorescence signal from the sample is collected by the same objective, passes through the beam splitter and is filtered by the second AOTF. An electronically switchable mirror directs fluorescence signal either to the photomultiplier tube (PMT) (in the fast scanning mode) or to the CCD camera (in the imaging mode) for detection.

A list of the proposed major equipment required to build a high-performance scanner includes: tunable AOTF filters TEAF7-. 40-. 65 (excitation channel) and TEAF7-. 45-. 70 (emission channel) (Brimrose Corporation of America, MD), switching time ∼1 μs, aperture 7×7 mm; an XY-stage, 70× 105 mm; an electromechanical translational stage MAX203B-NIK (Thorlabs, New Jersey) capable of simultaneously moving four standard sample slides (22×60 mm each) at a 10 mm/s speed with a 1 μm accuracy; a photomultiplier tube (PMT) R5900U-20-M4 (Hamamatsu Photonics, Inc.), spectral range 300 to 920 nm; a high-resolution CCD camera C9100-02 (Hamamatsu Photonics), pixel size 8×8 μm, electron multiplication gain 6× to 2000×, readout speed 30 to 520 frames/s, resolution 14 bit; a pigtailed light source iBeam smart (TOPTICA Photonics Inc., New York) providing the highest power in its class in the spectral range 300 to 800 nm and $a < 0.5\%$ power drift within 48 h, or a set of several laser sources supplied with a laser line combiner.

A limiting factor of fast scanning is the speed at which slides, mechanically translated on the stage above the objective, can be moved in the lateral plane without a drift from the focal plane. An imaging spot in the 10× objective is characterized by a 1.2×1.2 mm^2 field of view. At this size of the imaging

spot, the beam has to travel on the slide for a total length of 1100 mm $(22\ \text{mm}/1.2\ \text{mm}) \times 60\ \text{mm} = 1100\ \text{mm})$ to cover the entire area. Therefore, it takes approximately 2 min to scan the 1.44 mm^2 light spot over the entire slide $(1100\ \text{mm}/(10\ \text{mm}/s) = 2\ \text{min})$, if no stop requested. A time interval needed for autofocusing, testing and adjusting time exposures in different channels and collecting six high-resolution images at a particular area on the slide is approximately 2 s/spot. Therefore, according to these estimations a total time for scanning the entire slide and collecting six images in 100 selected spots (a higher number of clinically relevant CECs on the slide) is expected not to exceed 60 min/slide. A typical immunofluorescence assay targeting a single population of rare cells usually applies only three different fluorescent markers. Respectively, imaging in three spectral channels reduces scanning time to approximately 20 min/slide.

It is interesting to contrast performance of the intelligent search principle proposed here with the sequential imaging principle as used in the conventional flow cytometers and laser scanners. For example, when the slide scanning is performed using the 10×, 0.45 NA objective and a 0.81 mm^2 imaging spot, the theoretically required minimal number of images to cover the entire slide area is $22 \times 67 = 1474$ (in a single spectral channel). In practice, however, the number of required images typically increases due to the limitations imposed by a chip size of the CCD and requirement of partial overlapping imaging areas at the image boundaries to exclude cell loss at the boundaries. Additionally, the scanner has to perform autofocusing in several pre-set raster points on the slide to eliminate possible image blurring due to the focal drift during the slide movement. As recently reported for the state-of-the-art digital scanner widely used in the CTCs detection, each slide is scanned at 10× magnification in three channels and produces 6900 images.[15] The highest number of CTCs cells reported in that study was 199.3 ml^{-1}, with a range of 1.4 to 199.3 ml^{-1} CTCs detected in different samples. Typically, one slide can hold approximately 0.7 to 1 ml of cell suspension. If 1 ml of the sample containing 199.3 ml^{-1} rare cells is deposited on the single slide, that would require imaging at 200 areas on the slide and collecting a total of 600 images in three spectral channels to capture all target cells. Therefore, this example demonstrates that by applying the intelligent search principle on the same scanning instrument, one can reduce a required number of images approximately 10-fold, without compromising accuracy of target cell detection.

4 System Verification in Test Experiments

To validate feasibility of the proposed dual-mode scanning approach for rare cell detection, we performed a series of proof-of-concept experiments. In these tests, a blood sample from a healthy donor was spiked with human umbilical vein endothelial cells (HUVEC). HUVEC cells closely resemble molecular and morphological characteristics of circulating endothelial cells and are often used as a model system for CECs. As a negative control, we used a blood sample not enriched with HUVEC cells.

In these experiments, we added HUVEC cells to blood samples in the controlled amounts and tested how many of these target cells can be detected on the slides using our scanning approach. The blood samples collected from healthy donors were purchased from a commercial vendor and processed following procedure described earlier.[13] Specifically, after performing a white blood cell count, 4 ml of blood was distributed into several individual vials, each of which was enriched with 50, 100 or 400 HUVEC cells, respectively. HUVEC cells were counted and suspended in a small volume of the incubation buffer before addition to the blood samples. In a separate vial, the same amount of blood was added without enrichment as a negative control. All blood samples were lysed using ammonium-chloride-potassium (ACK) lysing buffer (Lonza Walkersville, Inc.) for 5 min. After lysis, the white blood cell pellets in each vial were resuspended in 8 ml of house-made isotonic imaging buffer and evenly deposited on the adhesive slides (Marienfeld, Bad Mergentheim, Germany[9]) at 1 ml per slide. Calculated density of the white blood cells on the slide was approximately 3.5×10^6 cells. After incubation on the slides for sufficient adherence (40 min, 37°C), the cells were fixed and immunostained with a corresponding set of antibodies. We used mouse monoclonal CD146 antibody (P1H12 Abcam Inc., Cambridge, Massachusetts) as a marker for HUVEC cells and secondary fluorescently labeled anti-mouse Alexa Fluor-555 antibody (Invitrogen Inc., Carlsbad, California) to visualize distribution of this marker. Optimal immunostaining and imaging conditions adjusted for the lowest expression level of the CD146 marker were established in the prior experiments when only HUVEC cells at different proliferation stages were deposited on the slides. For visualizing leukocytes, we used CD45:Alexa Fluor-647 conjugate antibody (AbD Serotec Inc., Raleigh, North Carolina) as a generally recognized specific marker of the white blood cells. DAPI nuclear stain (Invitrogen Inc., Carlsbad, California) was used to visualize nuclei in all cells and perform a total cell count.

All eight slides from each enrichment series were scanned on the iMIC digital microscope (TILL Photonics Inc., Germany) equipped with QImaging Retiga 2000DC cooled interline CCD (1600 × 1200 pixels) and a laser line combiner aligning together excitation beams from 532 and 647 nm diode pumped lasers (CrystaLasers, Inc). The microscope was equipped with the 10×, 0.45 N.A. and 20×, 0.75 N.A. Nikon Plan Apochromat objectives. Excitation and fluorescence signals were separated using a 9-filter "Sedat" quad-band set DA/FI/TR/Cy5-4X4M-B (Semrok Inc., Rochester, New York).

Obtained sets of three-color images were fed to the image analysis software. All potential hits generated by automatic analysis were manually inspected for final cell identification. Although not absolute, several physical properties distinguish CECs from the rest of normal blood cells. These include a larger size of most endothelial cells, a larger nucleus size and a clearly expressed cytoplasm surrounding intact nuclei. These cells express endothelial markers such as CD146 and do not express CD45. In our search criteria, we defined target cells as DAPI + CD146 + CD45− ("blue"-"green"-"no red") cells having the larger size (>15 μm), extensive cytoplasm, and the larger nucleus size (>8 μm) as opposite to smaller DAPI + CD146 − CD45+ ("blue"-"no green"-"red") leukocytes. Representative images containing target HUVEC cells are shown in Fig. 3. An obtained cell distribution pattern clearly demonstrates that HUVEC cells can be easily discriminated from the white blood cells by their morphological differences and expression of specific markers.

In average, we detected approximately $(3.40 \pm 0.05) \times 10^6$ leukocytes per slide as counted by the number of intact nuclei. In the corresponding dilution series with 50, 100 and 400 HUVEC cells added to the blood samples, we retrieved 43, 91 and 389

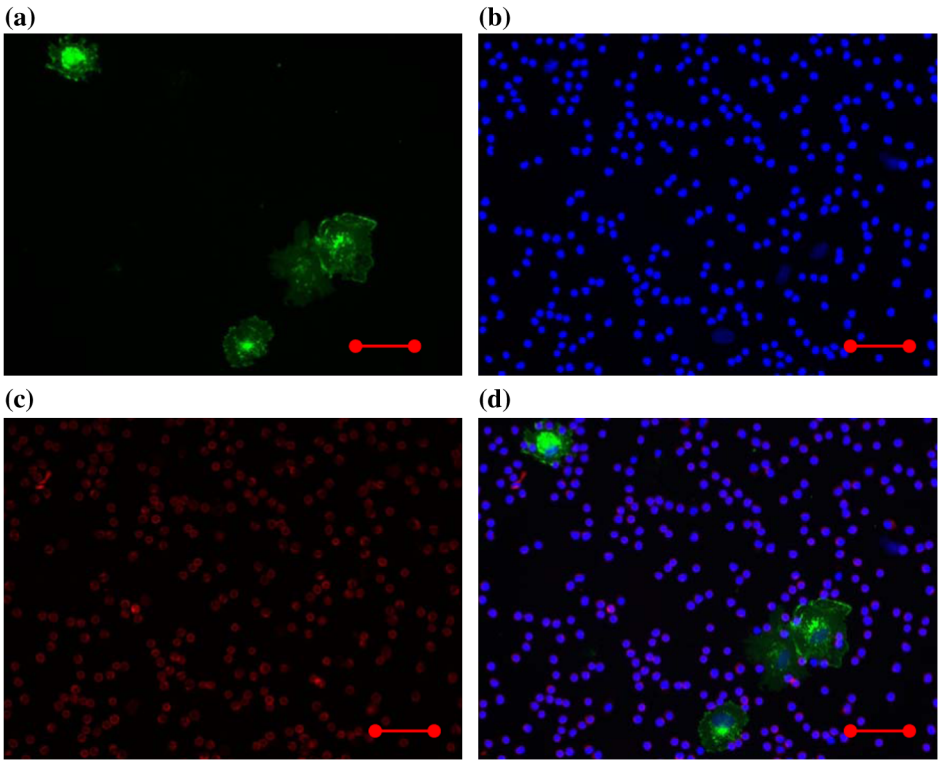

Fig. 3 Pilot experiments demonstrate that target cells of interest can be discriminated from the leukocytes using the proposed technology. The sample containing white blood cells, enriched with a small amount of HUVEC cells was scanned using a proposed principle. Images collected in the three spectral channels at the designated area on the slide show typical distributions of (a) Alexa Fluor-555 (green), (b) DAPI (blue), and (c) Alexa Fluor-647 (red) fluorescent markers, respectively. The images were superimposed for comparison (d). HUVEC cells are clearly distinguishable among the white blood cells as CD146 + CD45− cells of a larger size, with bigger nuclei and a larger cytoplasm/nuclear areas ratio. Leukocytes are CD45+ cells of a smaller size, having a smaller cytoplasm/nuclear ratio. Scale bar corresponds to 20 μm on (a)–(d), respectively.

target cells, respectively, which correspond to 86%, 91% and 97% rare cell recovery. Interestingly, the target cells from enrichment were distributed rather uniformly on the slides in each dilution series, and were not seen to form observable clusters. For instance, in the experiment with the sample enriched with 50 ml^{-1} of HUVEC cells, hits were distributed at the density of 41 to 54 cells/slide (each slide accommodated 1 ml of the solution). In the negative control experiments with the blood sample not containing HUVEC cells, the scanner identified some false positive hits, typically between 5 and 12 on the individual slides. These images contained false bright objects such as dye aggregates stuck on the slide surface. Approximately the same numbers of false positive hits were also detected on the slides enriched with HUVEC cells. A washing protocol can be further optimized to reduce dye aggregates on the slides. This will improve a general performance of the system and optimize a total operational time.

Finally, we evaluated performance of the dual-mode scanning against the sequential imaging scanning through the set of experiments, in which two slides from the same sample preparation were scanned by either of the methods. The blood sample used in these experiments was enriched with 50 ml^{-1} of HUVEC cells; 1 ml of cell suspension was deposited on each slide. The sequential imaging mode was programmed according to the algorithm as described earlier.[13,15] In the sequential mode, the instrument collected 6912 images in three channels and completed a scanning cycle in 110 min. The subsequent digital image analysis counted $(3.20 \pm 0.05) \times 10^6$ nucleated cells on the slide and identified 44 target cells among them. In the dual-mode scanning, the entire operational cycle (slide scanning and data analysis) was completed within 30 min. The results showed 43 target cells and six false positive hits on the slide. Hence, these data clearly demonstrate that the intelligent scanning principle offers a significant gain in speed while providing the same accuracy of rare cell detection as compared to the sequential scanning mode.

5 Summary

To be routinely implemented in clinical practice, the current technological platforms for rare cell detection need significant optimization. Among other approaches, enrichment-free imaging strategies for rare cell detection offer considerable advantages of not relying on any single protein marker and instead exploiting a range of markers and distinct morphological features for target cell identification. A conventional imaging flow cytometry implies that each slide is scanned entirely, and a resulting series of multicolor images is used for further analysis. The cycles of recording and analyzing sets of images in the numerous areas on the slide that do the not contain cells of interest (CECs in this case) reduce the efficiency of the instrument. This unproductive operational mode makes a running time to complete a single round of analysis exceedingly long. To overcome this shortage, we developed and validated the intelligent search principle that can be used in any digital imaging scanner and optimizes its performance for detecting rare cells. The search principle implemented in the proposed dual-mode multi-spectral imaging scanner exploits the scarcity of rare cells. The instrument performs a fast scanning of the entire

slide by a narrow single beam, which gives a signal triggering an imaging mode only in the selected areas on the slide where potential target cells are spotted by their unique spectral signatures. In this way, the same accuracy of rare cell detection can be achieved at a significantly reduced time required for data collection and analysis.

In future studies, the technology will be further evaluated and optimized using blood samples from patients with compromised vasculature. These patients are known to have an elevated level of CECs in their blood circulation. In addition to detection of CECs, the proposed method can be applied to enumeration of any other type of rare cells (or their mixed populations) as long as these cells can be distinguished using the immunofluorescence principle. The method holds a potential for full automation of the entire operational cycle (sample preparation, scanning and data analysis) once specifications for complete automation and routine settings are established in pilot preclinical testing.

CECs have been detected in patients with various cardiovascular diseases. Their level correlates with vascular damage and dysfunction, and appears to be predictive of an impending heart attack or ischemic stroke. Because coronary artery biopsy is not possible in live patients, CECs provide an extraordinary window into evaluation of arterial disruption and healing, and serve as a fluid-phase biopsy. To realize their great promise as unique biomarkers in cardiovascular assessment, detection of CECs has to be routinely integrated in the clinical practice. The instrument for the CECs detection proposed here has been developed with the clinical environment in mind and can potentially provide a sensitive, fast, high-throughput and inexpensive tool to fill this great void.

6 Materials and Methods

6.1 *Blood Sample Processing and Slide Preparation*

Blood samples from healthy donors were purchased from AllCells, LLC., Emeryville, CA. The blood was collected via venipuncture in EDTA tubes, stored and delivered at 4°C. Before processing, a white blood cell count was performed using Scepter™ 2.0 cell counter. Red blood cells were eliminated from the sample by erythrocyte lysis in the ammonium chloride solution. The blood was mixed at 1:5 volume ratio with ACK lysing buffer (Lonza Walkersville, Inc.), incubated for 5 min at room temperature on the rocker and centrifuged at $200 \times g$ for 5 min. The white blood cells pellet was resuspended without washing in the house-made incubation buffer (50 mM NaCl, 5 mM KCl, 1 mM $MgCl_2$, 2 mM $CaCl_2$, 10 mM Hepes, 2 mg/ml glucose, 330 mosm, pH 7.4). HUVEC cells were cultured as recommended by the supplier (Lonza Walkersville, Inc.). For using in spike experiments, the HUVEC cells were trypsinized, resuspended in phosphate buffered saline (PBS) buffer and counted using Hemacytometer by Tryptan Blue exclusion. A specific amount of HUVEC cells was added to resuspended white blood cells pellet in the tube and gently mixed using pipettes. Enriched white blood cells suspension was deposited on the adhesive slides (Marienfeld, Bad Mergentheim, Germany[9]) in the amount of 1 ml/slide. An estimated cell density on the slide was 3.5×10^6/slide. Slides were incubated at 37°C for 40 min for sufficient cell adhesion. At this stage, cells on the slides were ready for immunostaining.

6.2 *Immuno-Staining Conditions*

Cell fixation was performed with 2% PFA at room temperature for 20 min, followed by permeabilization using −20°C cooled methanol at room temperature for 5 min. Cells were pre-blocked with 10% goat serum in PBS at room temperature for 20 min. All antibodies were diluted to their working concentration in 10% goat serum PBS buffer. Antibody concentrations and incubation times were, respectively: CD146 (P1H12) at 1:250 dilution (0.004 mg/ml), 37°C, 40 min; Alexa Fluor-555 at 1:500 dilution (0.004 mg/ml), 37°C, 20 min; CD45:Alexa Fluor-647 at 1:125 dilution, 37°C, 40 min; DAPI at 1:1000 dilution, room temperature, 1 min.

References

1. T. R. Ashworth, "A case of cancer in which cells similar to those in the tumours were seen in the blood after death," *Aust. Med. J.* **14**, 146–147 (1869).
2. J. Kaiser, "Medicine. Cancer's circulation problem," *Science* **327**(5969), 1072–1074 (2010).
3. M. Yu et al., "Circulating tumor cells: approaches to isolation and characterization," *J. Cell. Biol.* **192**(3), 373–382 (2011).
4. C. J. Boos, G. Y. Lip, and A. D. Blann, "Circulating endothelial cells in cardiovascular disease," *J. Am. Coll. Cardiol.* **48**(8), 1538–1547 (2006).
5. D. G. Duda et al. "Differential CD146 expression on circulating versus tissue endothelial cells in rectal cancer patients: implications for circulating endothelial and progenitor cells as biomarkers for antiangiogenic therapy," *J. Clin. Oncol.* **24**(9), 1449–1453 (2006).
6. F. Sabatier et al., "Circulating endothelial cells, microparticles and progenitors: key players towards the definition of vascular competence," *J. Cell. Mol. Med.* **13**(3), 454–471 (2009).
7. E. Shantsila, A. D. Blann, and G. Y. Lip, "Circulating endothelial cells: from bench to clinical practice," *J. Thromb. Haemost.* **6**(5), 865–868 (2008).
8. D. M. Smadja et al., "Circulating endothelial cells: a new candidate biomarker of irreversible pulmonary hypertension secondary to congenital heart disease," *Circulation* **119**(3), 374–381 (2009).
9. R. T. Krivacic et al., "A rare-cell detector for cancer," *Proc. Natl. Acad. Sci. USA* **101**(29), 10501–10504 (2004).
10. A. Woywodt et al., "Isolation and enumeration of circulating endothelial cells by immunomagnetic isolation: proposal of a definition and a consensus protocol," *J. Thromb. Haemost.* **4**(3), 671–677 (2006).
11. S. Nagrath et al., "Isolation of rare circulating tumour cells in cancer patients by microchip technology," *Nature* **450**(7173), 1235–1239 (2007).
12. M. C. Miller, G. V. Doyle, and L. W. Terstappen, "Significance of circulating tumor cells detected by the cellsearch system in patients with metastatic breast colorectal and prostate cancer," *J. Oncol.* **2010**, 617421 (2010).
13. D. Marrinucci et al., "Case study of the morphologic variation of circulating tumor cells," *Hum. Pathol.* **38**(3), 514–519 (2007).
14. H. B. Hsieh et al., "High speed detection of circulating tumor cells," *Biosens. Bioelectron.* **21**(10), 1893–1899 (2006).
15. D. Marrinucci et al., "Fluid biopsy in patients with metastatic prostate, pancreatic and breast cancers," *Phys. Biol.* **9**(1), 016003 (2012).